Breakdown of avalanche critical behaviour in polycrystalline plasticity

THIEBAUD RICHETON, JÉRÔME WEISS* AND FRANÇOIS LOUCHET
Laboratoire de Glaciologie et Géophysique de l'Environnement, CNRS, 54 rue Molière, BP 96, 38402 St Martin d'Hères Cedex, France
*e-mail: weiss@lgge.obs.ujf-grenoble.fr

Published online: 8 May 2005; doi:10.1038/nmat1393

Acoustic emission experiments on creeping ice as well as numerical simulations argue for a self-organization of collective dislocation dynamics during plastic deformation of single crystals into a scale-free pattern of dislocation avalanches characterized by intermittency, power-law distributions of avalanche sizes, complex space-time correlations and aftershock triggering. Here, we address the question of whether such scale-free, close-to-critical dislocation dynamics will still apply to polycrystals. We show that polycrystalline plasticity is also characterized by intermittency and dislocation avalanches. However, grain boundaries hinder the propagation of avalanches, as revealed by a finite (grain)-size effect on avalanche size distributions. We propose that the restraint of large avalanches builds up internal stresses that push temporally the dynamical system into a supercritical state, off the scale-invariant critical regime, and trigger secondary avalanches in neighbouring grains. This modifies the statistical properties of the avalanche population. The results might also bring into question the classical ways of modelling plasticity in polycrystalline materials, based on homogenization procedures.

In crystalline materials with high dislocation mobility[1], the collective dislocation dynamics self-organize into a scale-free pattern of dislocation avalanches characterized by intermittency[2], power-law distributions of avalanche sizes[2,3], time correlations and aftershock triggering[4], as well as fractal distributions of avalanche locations and complex space-time coupling[5]. This is supported (i) by acoustic emission experiments on ice single crystals during creep, in which the amplitude A_0 of the acoustic bursts is a proxy of the strain dissipated during the avalanche, and (ii) by either discrete dislocation dynamics (DDD) simulations[2] or phase-field models[3].

These observations suggest that we should reconsider dislocation-related plasticity within a close-to-criticality non-equilibrium framework[2], reminiscent of the concept of self-organized criticality (SOC)[6]. They call into question the classical ways of modelling plasticity and plastic behaviour of materials, which use homogenization procedures. Indeed, such a scale-free intermittent pattern precludes the definition of an elementary representative volume over which a density of dislocations, an average velocity or an average strain rate can be defined.

However, the acoustic emission experiments carried out so far, as well as the numerical simulations quoted above, refer to single crystals in which complexity and multiscale properties solely arise from dislocations interacting through long-range elastic stresses. Most crystalline materials of structural and economical interest are polycrystalline: they are made of a very large number of small grains (from nanometres to centimetres) separated by grain boundaries. These boundaries are known to interact with dislocations during plastic deformation of polycrystals in many different ways. They act as strong barriers to dislocation motion, as evidenced by dislocation pile-ups that generate internal stresses (for instance in ice[7]). These internal stresses can activate pre-existing nearby dislocation sources in neighbouring grains[8], whereas actual dislocation transmission through a grain boundary is possible in some specific cases[9]. Grain boundaries can also act as effective dislocation sources[7,10]. In very fine-grained materials (that is, if the grain size is too small to allow the operation of Frank–Read sources), grain boundaries, which often act as dislocation sinks, can also serve as effective dislocation sources, as suggested by both scaling arguments[10,11] and molecular dynamics simulations. Interactions between dislocations and grain boundaries may be more complex when recrystallization processes,

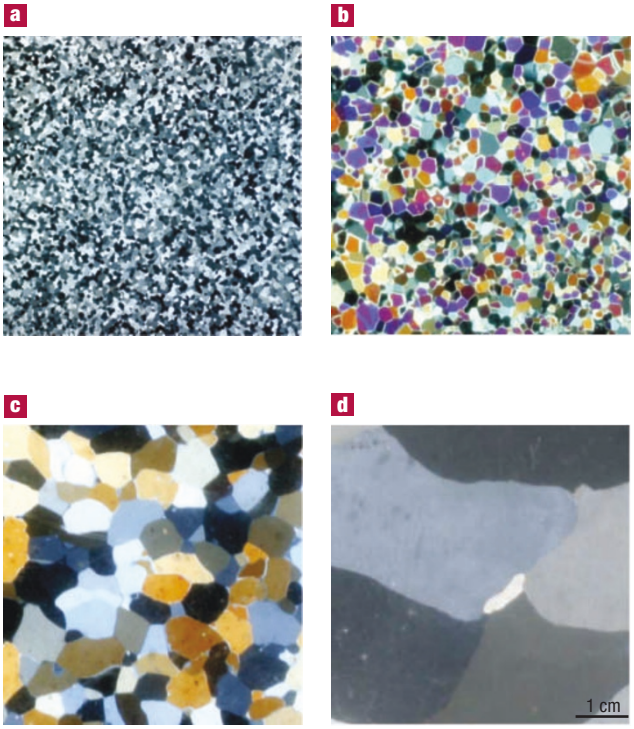

Figure1 Microstructures of the polycrystalline ice samples. Thin sections of four ice samples with different average grain sizes observed under cross-polarized light. **a**, Average grain size $\langle d \rangle$ = 0.26 mm, **b**, 0.87 mm, **c**, 1.92 mm, **d**, 5.02 mm.

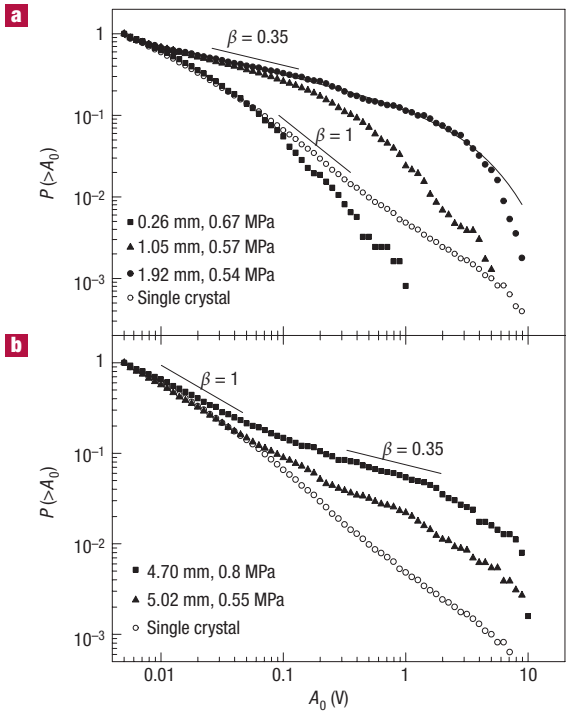

Figure 2 Distributions of dislocation avalanche sizes in polycrystals. Cumulative probability distributions for acoustic emission amplitudes in polycrystalline samples with different average grain sizes. All the tests were done at –10 °C. **a,** Fine-grained samples. The key shows the average grain size $\langle d \rangle$ and applied compression stress for three samples (closed symbols). Using a Levenberg–Marquardt algorithm, these distributions were fitted by the empirical relation $P(>A_0) \approx A_0^{-\beta}\exp(-A_0/A_c)$ to estimate the cut-off amplitude A_c. The fit is shown for the sample with $\langle d \rangle$ = 1.92 mm; thin black line. The cut-off A_c decreases with decreasing grain size, whereas the empirical exponent β is 0.35 ± 0.05 whatever the grain size. Because of relatively poor statistics (between 800 and 5,000 avalanches recorded for a test), a cumulative representation was preferred to better explore the high amplitudes. We checked from Monte Carlo simulations that this representation did not bias our estimation of the power-law exponent $\tau = \beta + 1$. These distributions are compared with a typical cumulative probability distribution for a single crystal showing no cut-off and an exponent $\tau = \beta + 1 = 2$ (open circles). **b**, Coarse-grained samples with bimodal distributions of grain sizes (closed symbols). The open circles represent a typical single-crystal cumulative probability distribution, given for reference. The distributions show a broken slope between a low-amplitude (β = 1) regime, and a high-amplitude (β = 0.35) regime. A limited cut-off is detectable only for very large amplitudes.

such as migration recrystallization, take place. This situation was not relevant in the present case, owing to the timescales involved. Moreover, we checked that the microstructure and the average grain size of our samples were the same before and after testing.

In this paper, we address the following question: will the scale-free, close-to-critical dislocation dynamics still apply to polycrystals? Grain boundaries acting as barriers to dislocation motion might indeed hinder large-scale propagation of dislocation avalanches, and mechanisms specific to polycrystals, such as grain-boundary-related dislocation sources, may modify the emerging pattern. To address this question, we recorded the acoustic emission during the plastic deformation of ice polycrystals with different average grain sizes and different grain size distributions, and we compared the statistical data to those obtained previously for single crystals[2]. Even if collective dislocation dynamics in single crystals has been successfully modelled by DDD[2] or phase-field[3] simulations, it is doubtful that such simulations could be performed for polycrystals without introducing some kind of simplified description of grain boundaries. Molecular dynamics simulations might indeed allow a correct description of interactions between grain boundaries and dislocation avalanches, but at a still unreachable computational cost.

We carried out compression creep (constant load) experiments on polycrystalline ice samples with an average grain size $\langle d \rangle$ varying from 260 μm to 5 mm (Fig. 1). These grain sizes are large compared with usual grain sizes of structural materials such as metals. Fine-grained (260 μm ≤ $\langle d \rangle$ ≤ 2 mm) samples were characterized by a unimodal, log-normal distribution of grain sizes, whereas two coarse-grained samples ($\langle d \rangle$ = 4.7 and 5.0 mm) were characterized by large grains (around 10 mm) embedded in a matrix of small grains (~1–2 mm). Most experiments were done at –10 °C, and one of them at –3 °C, much closer to the melting point. The applied stress varied between 0.54 and 0.80 MPa, that is, at least a factor of two below the threshold stress for microcrack nucleation in granular ice[13]. The applied total deformation ranged between 6×10^{-4} and 2×10^{-3}.

A piezoelectric transducer (frequency bandwidth 0.2– 1 MHz) was fixed on the samples. The amplitude range between the maximum and the minimum amplitude thresholds was 70 dB, that is, 3.5 orders of magnitude. For each event detected above the minimum threshold A_{min}, the acoustic emission system determined the maximum amplitude A_0, the arrival time t_0 and the duration δ.

Any acoustic emission analysis needs an acoustic source model to interpret the characteristics of the acoustic emission wave in terms

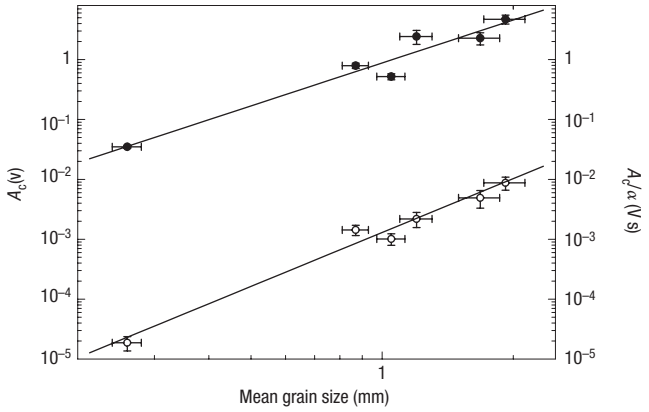

Figure 3 Grain-size effect on the dislocation avalanche sizes. Closed circles: relationship between the cut-off amplitude A_c of the probability distribution of avalanche sizes and the average grain size $\langle d \rangle$. In a log–log plot, a linear regression gives a slope of 2.4 ± 0.3, meaning that $A_c \propto \langle d \rangle^{2.4}$. We checked from Monte Carlo simulations that this scaling was not biased by the use of cumulative distributions (Fig. 2) to estimate A_c. Open circles: relationship between the ratio A_c/α, which is a proxy of the 'strained volume' Sb (see text for details) and the average grain size $\langle d \rangle$. A scaling $A_c/\alpha \propto \langle d \rangle^{3.0 \pm 0.2}$ is observed. Error bars represent one standard deviation.

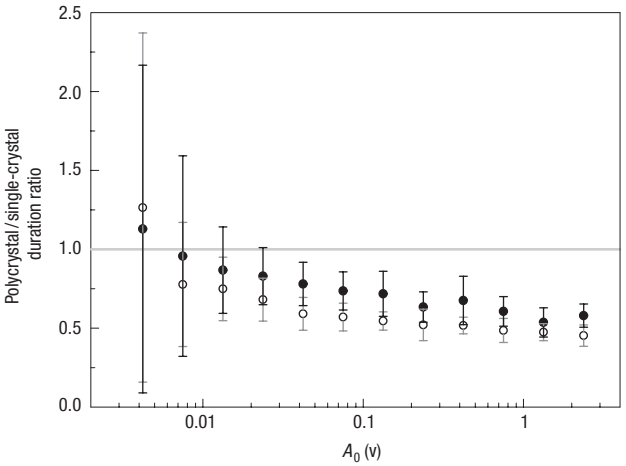

Figure 4 Avalanche durations in polycrystals. Ratio between the average duration of an event of amplitude A_0 in polycrystals and in a single crystal, as a function of A_0. Closed symbols: $\langle d \rangle = 5.02$ mm; applied stress 0.54 MPa. Open symbols: $\langle d \rangle = 1.92$ mm; applied stress 0.55 MPa. The average duration of an event decreases with decreasing average grain size, and the ratio decreases with increasing amplitude A_0. Error bars represent one standard deviation.

of a source mechanism. Following previous work[14], the amplitude of the acoustic wave for dislocation avalanches reads:

$$A(t) = \frac{3c_T^2}{4\pi c_L} \frac{\varphi b}{D^2} Lv = \frac{3c_T^2}{4\pi c_L} \frac{\varphi b}{D^2} \left(\frac{dS}{dt} \right)$$

where c_T and c_L are respectively the transverse and longitudinal wave velocities, ϕ is the material density, b the Burgers' vector, D the source–transducer distance, L the total dislocation length involved in the avalanche, and v the dislocation velocity (averaged over L). The quantity $dS/dt = Lv$ is therefore the area swept per unit time by dislocations. When multiplied by b and normalized by a volume, this term represents a strain rate, $d\varepsilon/dt$. An additional hypothesis is needed to estimate the strain increment dissipated by the avalanche. We assumed an exponential decay for the avalanche velocity, and therefore for the equivalent strain rate, $d\varepsilon/dt \approx (d\varepsilon/dt)_0 \exp(-\alpha(t - t_0))$. Then an integration of equation (1) over time gives

$$A_0 = \frac{3c_T^2}{4\pi c_L} \frac{\varphi \alpha}{D^2} Sb$$

Normalized by a volume, the term Sb represents a strain increment, whereas α is a damping coefficient. This decay hypothesis is supported (i) by the observed decay of $A(t)$ when the complete acoustic emission waves were recorded (during a single test), (ii) by the output of the DDD model detailed elsewhere[2], (iii) by good agreement between global acoustic emission activity and global deformation[15], and (iv) by a scaling of $\delta \propto \ln(A_0)$ that allows us to estimate the damping coefficient α (see Methods).

In single crystals of ice, collective dislocation dynamics self-organize into a scale-free pattern of dislocation avalanches characterized by intermittency with power-law distributions of avalanche sizes, $P(A_0) \propto A_0^{-\tau}$, the exponent $\tau = 2.0 \pm 0.05$ being independent of the driving stress[2]. Recent experiments revealed that τ is also independent of temperature[16]. This confirms the high degree of universality of the observed scaling, reminiscent of a critical behaviour.

Plasticity in polycrystalline samples is also characterized by intermittency and dislocation avalanches, despite a signature that significantly differs from the single-crystal scaling in two ways (Fig. 2a): (i) the observed power-law exponent, still independent of driving stress and temperature, is significantly smaller and independent of the average grain size; and (ii) a cut-off of this power-law scaling is observed towards large amplitudes. Note that for the finest-grained sample ($\langle d \rangle = 260$ μm), the power-law regime is not really observed, as the cut-off is noticeable down to small amplitudes, near the amplitude threshold. The cumulative distributions of avalanche size can be fitted by the empirical relation $P(>A_0) \approx A_0^{-\beta} \exp(-A_0/A_c)$, with $\beta = \tau - 1 = 0.35 \pm 0.05$. The cut-off function introduces a characteristic scale A_c that can be linked to the microstructural characteristic scale, that is, the average grain size, $\langle d \rangle$. The smaller the grain size, the smaller the cut-off amplitude. As deduced from a fitting procedure, A_c scales as $\langle d \rangle^{2.4 \pm 0.3}$ (Fig. 3). In the case of coarse-grained samples with bimodal distributions of grain sizes, we observed a broken slope in the power-law regime: an exponent $\beta = 1$ (that is, $\tau = 2$, the signature of single crystals) is recovered at small amplitudes whereas $\beta = 0.35$ is observed at larger scales (Fig. 2b).

The grain-size effect documented on Figs 2 and 3 illustrates the role of grain boundaries as barriers to the dynamical propagation of dislocation avalanches, and arises from the total dislocation length L that can be involved in the avalanche (equation (1)). On average, L cannot be larger than the dislocation length that can be mobilized for dislocation motion within a grain. We found that this quantity scaled as $\langle d \rangle^{2.4}$. Grain boundaries are also more directly a barrier to dislocation propagation, as evidenced by a comparison between avalanche durations in single crystals and polycrystals (Fig. 4). For a given amplitude A_0, which is from equation (1) a proxy of the initial avalanche spreading rate $(dS/dt)_0$, δ is, on average, smaller in polycrystals than in single crystals, and decreases with decreasing grain size. In other words, the smaller the grain size, the quicker the avalanches are damped. Moreover, this difference between single and polycrystals increases with increasing amplitude A_0: that is, the effect

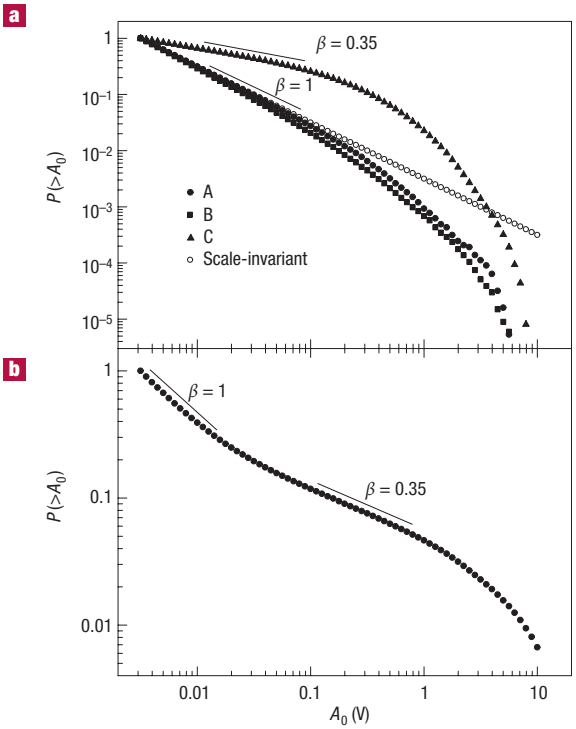

Figure 5 Distributions of avalanche sizes in Monte Carlo simulations. a, Unimodal grain-size distributions (corresponding to fine-grained samples of Fig. 2a). Results of Monte Carlo simulations A, B and C (closed symbols) expressed in terms of cumulative amplitude distributions. This cumulative representation has been chosen for a direct comparison with Fig. 2, but a probability density representation leads to the same conclusions. These simulations are compared to a perfect scale-invariant $P(>A_0) \propto A_0^{-1}$ distribution (open circles). **b**, Bimodal grain-size distribution (corresponding to coarse-grained samples of Fig. 2b). The broken slope observed on Fig. 2b is recovered.

of grain boundaries is stronger for large avalanches, as they interact more systematically with the boundaries than small avalanches. The combination of these two effects, on the length of dislocation that can be mobilized and on dislocation propagation, suggests that an avalanche cannot spread, on average, over more than the grain volume. Indeed, we observed that the ratio A_c/α, which scales as a 'strained volume' Sb (equation (2)), scales as $\langle d \rangle^{3.0\pm0.2}$ (Fig. 3). The introduction of a microstructural scale, the average grain size, leaves its fingerprint on the dynamics of plastic deformation by hindering the emergence of the scale-free critical pattern.

Although the polycrystalline microstructure consistently explains the cut-offs in the avalanche size distributions, the change of the power-law exponent has no trivial explanation. In critical dynamical systems, critical exponents depend only on a few fundamental parameters such as the effective dimensionality and the basic symmetries of the system, and not on microscopic details related to the individual behaviour of the interacting entities[17]. In our case, this would imply that the acoustic emission waves recorded in polycrystals are related to a different deformation mechanism from that in single crystals. We recall that twinning does not occur in ice and that we applied stresses well below the microcrack nucleation threshold, thus eliminating these potential acoustic emission sources. Subcritical cracking might be another possible source of acoustic emission, as observed in rocks[18]. However, in such a case, acoustic emission activity should increase with increasing deformation (that is, increasing crack length), whereas we observed a decrease of acoustic emission activity as the material hardened (that is, the viscoplastic strain rate decreased).

We propose here an alternative explanation for the change of the exponent, which may result from a complex combination of the development of internal stresses, aftershock triggering and grain-size statistics. We carried out three types of simple Monte Carlo simulations in which primary avalanches are randomly selected within a power-law distribution of avalanche amplitudes, $P(A_0) \propto A_0^{-\tau}$, with $\tau = 2$, that is, the single-crystal scaling.

Simulation A: each avalanche is ascribed randomly to a grain of size d selected within a log-normal distribution of grain sizes. Following our observations, a cut-off amplitude A_c scaling as $d^{2.4}$ is associated with this grain. If $A_0 < A_c$, the avalanche is 'accepted' into a new distribution of avalanche sizes, meaning that the avalanche mobilized an acceptable total dislocation length L. If $A_0 \geq A_c$, the avalanche is simply discarded. This first simulation is limited to this very crude finite-size effect, meaning that each grain is assumed to be an isolated system, independent of the neighbouring grains. Not surprisingly, this simulation reproduces a cut-off but not a decrease of the power-law exponent (Fig. 5a).

Simulation B: it is certainly incorrect to assume that each grain is an isolated system. Instead, it is fair to assume that when an avalanche is restrained by grain boundaries, the dislocations that have piled up against the boundaries generate an internal stress σ_{int} within the neighbouring grains. This adds to the applied external stress σ_{ext} to drive plastic deformation in such grains, in agreement with X-ray topography observations[7,8]. In our simulations, we further assume that (i) σ_{int} is proportional to $A_0 - A_{th}$, where the threshold A_{th} is itself defined as a (small) fraction of A_c and therefore scales as $d^{2.4}$ (the larger the avalanche amplitude compared with the grain volume, the larger the internal stress); and (ii) this increased driving triggers an excess of dislocation avalanches within other grains (to which are also ascribed different grain sizes selected among the log-normal distribution). It is implicitly assumed that those grains are neighbours, although topology is ignored in these Monte Carlo simulations. For the sake of simplicity, the amplitude (or strain, see relation (2)) cumulated over these triggered avalanches ('aftershocks') is assumed to be proportional to σ_{int}. If large enough compared with the volume of the grain where they have been triggered, these aftershocks can in turn generate internal stresses and so secondary aftershocks. This cascade stops after a few steps, as the cumulated triggered amplitude is smaller than the amplitude of the mother avalanche. In simulation B (Fig. 5a), the amplitudes of these aftershocks are selected among the power-law distribution ($\tau = 2$): as for single crystals[4], the aftershock population is supposed to belong to the global avalanche population characterizing the critical dynamics. With this distribution of aftershock amplitudes, it is implicitly assumed that the conditions for the emergence of a scale-free critical dynamics still prevail within each grain. However, simulation B does not show a decrease of the exponent (Fig. 5a).

Simulation C: here, we propose that the sudden and local development of internal stresses resulting from the restraint of a large avalanche breaks down one of the main necessary conditions for SOC, that is, an external driving rate much slower than the internal relaxation processes[19]. The additional driving rate $d\sigma_{int}/dt$ is by nature of the same order of magnitude than the relaxation processes (avalanches), therefore pushing temporally the local system (the neighbouring grain) out of the marginally stable state. In this transient supercritical state, the system is forced to relax strain through a single large avalanche (see previous work[20] for the connection between large driving rates and a supercritical state). In simulation C, this is described by a single aftershock of amplitude $A_0 - A_{th}$ which is ascribed to a grain selected within the log-normal distribution. Once again, if large enough compared with the grain

volume, this aftershock might itself generate internal stresses and trigger secondary aftershocks, and so on. Simulation C reproduces a cut-off at large scales that depends on the average grain size, as well as a decrease of the power-law exponent (Fig. 5a). In this model, in spite of having an apparent power-law scaling over a limited scale range, the observed exponent does not characterize a critical state, but instead results from a complex combination of (i) a close-to-critical state (with $\tau = 2$) occurring within each grain, (ii) the development of internal stresses that drive neighbouring grains into a transient supercritical regime and (iii) a distribution of grain sizes. In simulation C, the observed exponent decreases with decreasing the ratio A_{th}/A_c, that is, with an increasing amount of triggered aftershocks (consequently, the agreement between the value of β in Fig. 5a and the experimental value should not be given too much weight, as the ratio A_{th}/A_c cannot be estimated from experiments). This model is further supported by simulations introducing a bimodal grain-size distribution. In agreement with experiments, a broken slope is obtained in the power-law regime, from $\tau = 2$ at small scales to $\tau < 2$ at larger scales (Fig. 5b). A time clustering of avalanches—that is, some aftershock activity—was observed during our experiments on polycrystals. The population of clustered events seemed to show a slight deficit of large avalanches compared with the total population, but the limited statistics did not allow us to pursue the analysis further.

The results of simulation C are also supported by the result of an additional creep test on a polycrystal with $\langle d \rangle = 2.6$ mm, for which the use of six transducers allowed us to locate the avalanches spatially in three dimensions. We observed that the avalanches were spatially correlated over distances at least one order of magnitude larger than the average grain size, therefore invalidating a simple cut-off effect such as the one of simulation A (unpublished work). Details of localization methods and correlation analysis have been published previously[5].

This work shows that polycrystalline plasticity can display intermittency and avalanche phenomena, although the scale-free pattern observed in single crystals is disturbed by the introduction of a microstructural scale, the average grain size. This grain-size effect is not a simple, trivial finite-size effect, as grain boundaries act as barriers to the dynamic propagation of avalanches but also transmit internal stresses. If the scheme proposed in simulation C is correct, it calls into question the modelling of polycrystalline plasticity by classical micro–macro approaches such as homogenization. A trivial finite-size effect, such as the one in simulation A, could validate homogenization procedures in polycrystals if the representative volume is significantly larger than $\langle d \rangle$. However, the aftershock triggering detailed in simulation C would mean that the intermittent and localized character of plastic deformation extends towards scales much larger than the average grain size, in agreement with the long-range spatial correlations reported above.

METHODS

AVALANCHE DURATION AND DAMPING:

For each event, the acoustic emission recording system defines the duration as $\delta = t_e - t_0$, where t_0 is the arrival time, that is, the time at which the signal goes beyond the amplitude detection threshold A_{min} (3×10^{-3} V, or 30 dB, in our case), and t_e is the time after which the signal remains below A_{min} during more than a fixed duration (100 μs in our case). Assuming an exponential decay for the avalanche spreading rate dS/dt in equation (1), we have

$A_e = A_{min} = A_0 \exp[-\alpha(t_e - t_0)]$

which leads to

$\delta = t_e - t_0 = (\ln A_0 - \ln A_{min})/\alpha$

This allows us to estimate the damping coefficient α from the scaling $\delta \propto \ln A_0$.

Received 2 December 2004; accepted 11 April 2005; published 8 May 2005.

References

1. Zaiser, M. & Seeger, A. in *Dislocations in Solids* (eds Nabarro, F. R. N. & Duesbury, M. S.) 1–100 (Elsevier, Amsterdam, 2002).
2. Miguel, M. C., Vespignani, A., Zapperi, S., Weiss, J. & Grasso, J. R. Intermittent dislocation flow in viscoplastic deformation. *Nature* **410,** 667–671 (2001).
3. Koslowski, M., LeSar, R. & Thomson, R. Avalanches and scaling in plastic deformation. *Phys. Rev. Lett.* **93,** 125502 (2004).
4. Weiss, J. & Miguel, M.-C. Dislocation avalanche correlations. *Mater. Sci. Eng. A* **387–389,** 292–296 (2004).
5. Weiss, J. & Marsan, D. Three dimensional mapping of dislocation avalanches: clustering and space/time coupling. *Science* **299,** 89–92 (2003).
6. Bak, P., Tang, C. & Wiesenfeld, K. Self-organized criticality. *Phys. Rev. A* **38,** 364–374 (1988).
7. Liu, F. & Baker, I. Dislocation-grain boundary interactions in ice crystals. *Phil. Mag. A* **71,** 15–42 (1995).
8. Baillin, X., Pelissier, J., Bacmann, J. J., Jacques, A. & George, A. Dislocation transmission through $\Sigma = 9$ symmetrical tilt boundaries in silicon and germanium. I. In situ observations by synchrotron X-ray topography and high-voltage electron microscopy. *Phil. Mag. A* **55,** 143–164 (1987).
9. Baillin, X., Pelissier, J., Jacques, A. & George, A. Direct evidence of dislocation transmission through $\Sigma = 9$ grain boundaries in germanium and silicon by in situ high-voltage electron microscopy observations. *Phil. Mag. A* **61,** 329, 362 (1990).
10. Louchet, F. in *7th Int. Symp. Plasticity and its Current Applications* (ed. Khan, A. S.) 585–588 (NEAT Press, Fulton, Maryland, 1999).
11. Louchet, F. & Kung, H. On the Hall–Petch law breakdown in nanocrystalline materials. *J. Metastable Nanocryst. Mater.* **7,** 55–63 (2000).
12. van Swygenhoven, H. Grain boundaries and dislocations. *Science* **296,** 66–67 (2002).
13. Frost, H. J. Mechanisms of crack nucleation in ice. *Eng. Fracture Mech.* **68,** 1823–1837 (2001).
14. Rouby, D., Fleischman, P. & Duvergier, C. Un modèle de source d'émission acoustique pour l'analyse de l'émission continue et de l'émission par salves: I. Analyse théorique. *Phil. Mag. A* **47,** 671–687 (1983).
15. Weiss, J. & Grasso, J. R. Acoustic emission in single crystals of ice. *J. Phys. Chem.* **101,** 6113–6117 (1997).
16. Richeton, T., Weiss, J. & Louchet, F. in *Proc. 2nd Int. Conf. Multiscale Materials Modeling* (ed. Ghoniem, N. M.) 239–241 (Los Angeles, California, 2004).
17. Stanley, H. E. Scaling, universality, and renormalization: The three pillars of modern critical phenomena. *Rev. Mod. Phys.* **71**, S358–S366 (1999).
18. Main, I. G., Sammonds, P. R. & Meredith, P. G. Application of a modified Griffith criterion to the evolution of fractal damage during compressional rock failure. *Geophys. J. Int.* **115,** 367–380 (1993).
19. Jensen, H. J. *Self-Organized Criticality* (Cambridge Univ. Press, Cambridge, 1998).
20. Main, I. Statistical physics, seismogenesis, and seismic hazard. *Rev. Geophys.* **34,** 433–462 (1996).

Acknowledgements

We thank M. C. Miguel for providing us the output data of her model, and A. Manouvrier for technical assistance.

Correspondence and requests for materials should be addressed to J.W.

Competing financial interests

The authors declare that they have no competing financial interests.